Rapid analysis of gravity changes after the Mw 8.2 Chignik earthquake from GRACE Follow-On intersatellite laser ranging measurements

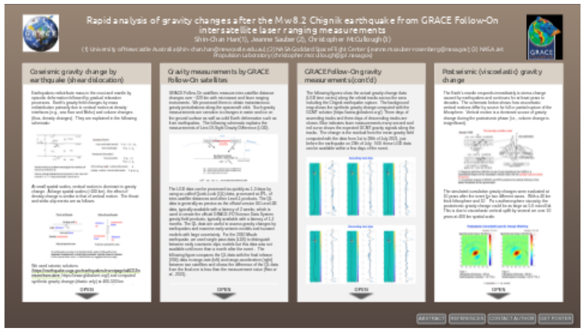

Shin-Chan Han(1), Jeanne Sauber(2), Christopher McCullough(3)

(1) University of Newcastle Australia (shin-chan.han@newcastle.edu.au); (2) NASA Goddard Space Flight Center (jeanne.m.sauber-rosenberg@nasa.gov); (3) NASA Jet Propulsion Laboratory (christopher.mccullough@jpl.nasa.gov)

PRESENTED AT:

COSEISMIC GRAVITY CHANGE BY EARTHQUAKE (SHEAR DISLOCATION)

Earthquakes redistribute mass in the crust and mantle by episodic deformation followed by gradual relaxation processes. Earth's gravity field changes by mass redistribution primarily due to vertical motion at density interfaces (e.g., sea floor and Moho) and volume changes (thus, density changes). They are explained in the following schematic:

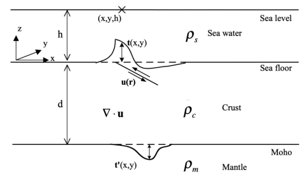

Vertical motion (up-/down-warping) at the interface of density stratification $\mathbf{u}$

Volume change (dilatation/compression) in the crust and mantle $\nabla \cdot \mathbf{u}$ => "long wavelength" phenomena

Coseismic (Elastic)

Long wavelength (spatial) $\nabla \cdot \mathbf{u} \approx$ or $> \mathbf{u}_z$

Short wavelength $\nabla \cdot \mathbf{u} \ll \mathbf{u}_z$

Postseismic (Viscoelstic)

~incompressible $\nabla \cdot \mathbf{u} \approx 0$

$\nabla \cdot \mathbf{u} \ll \mathbf{u}_z$

GPS, leveling, InSAR = surface deformation $\mathbf{u}$

Gravity = surface + interior deformation $\nabla \cdot \mathbf{u}$ & $\mathbf{u}_z$

At small spatial scales, vertical motion is dominant in gravity change. At large spatial scales (>100 km), the effect of density change is similar to that of vertical motion. The thrust and strike-slip events are as follows:

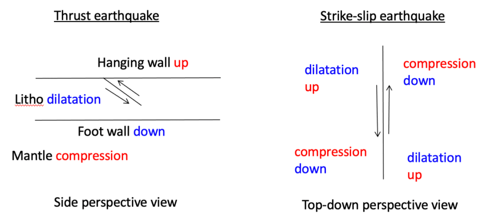

An earthquake occurring in an idealized elastic region is followed by time-dependent readjustment as underlying viscoelastic material relaxes in response to the imposed static stress => Deformation w/ negligible density change.

We used seismic solutions (https://earthquake.usgs.gov/earthquakes/eventpage/ak0219neiszm/executive; (https://gcc02.safelinks.protection.outlook.com/?url=https%3A%2F%2Fearthquake.usgs.gov%2Fearthquakes%2Feventpage%2Fak0219neiszm%2Fexecutive&data=04%7C01%7Cjeanne.m.sauber-rosenberg%40nasa.gov%7C6529f441c71d46bd998808d9b90a211a%7C7005d45845be48ae8140d43da96dd17b%7C0%7C0%7C637744275430757605%7CUnknown%7CTWFpbGZsb3d8eyJWIjoiMC4wLjAwMDAi%3D%7C3000&sdata=0k7VT9glqEjhf8XZkvETSMZbP6eOH34YGzSf7Z3IaYk%3D&reserved=0)https://www.globalcmt.org/) and computed synthetic gravity change (elastic only) at 400-500 km resolution below using the code discussed in *Broese et al.,* (2015):

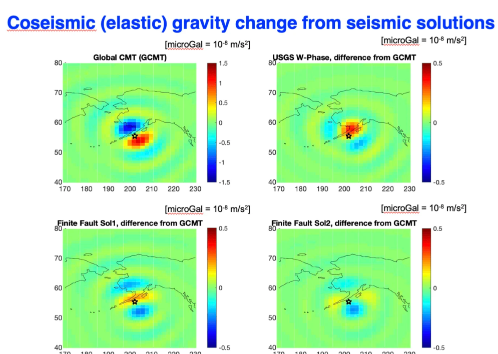

GRAVITY MEASUREMENTS BY GRACE FOLLOW-ON SATELLITES

GRACE Follow-On satellites measure inter-satellite distance changes over ~220 km with microwave and laser ranging instruments. We processed them to obtain instantaneous gravity perturbations along the spacecraft orbit. Such gravity measurements are sensitive to changes in water and ice on the ground surface as well as solid Earth deformation such as from earthquakes. The following schematic explains the measurements of Line-Of-Sight Gravity Difference (LGD).

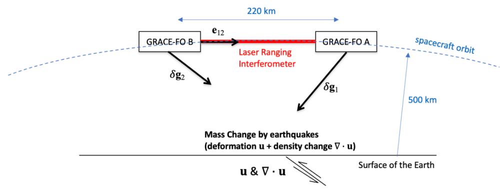

$\delta\mathbf{g}_1$ ... gravity vector exerted by water on GRACE-FO A
$\delta\mathbf{g}_2$ ... gravity vector exerted by water on GRACE-FO B
$\mathbf{e}_{12}$ ... line-of-sight (LOS) unit vector

$\delta g_{12}^{LOS} = (\delta\mathbf{g}_1 - \delta\mathbf{g}_2) \cdot \mathbf{e}_{12}$ ... **Line-of-sight Gravity Difference (LGD)**

The LGD data can be processed as quickly as 1-3 days by using so-called Quick-Look (QL) data, processed at JPL, of inter-satellite distances and other Level-1 products. The QL data is generally as precise as the official version 04 Level-1B data, typically available with a latency of 2 weeks, which is used to create the official GRACE-FO Science Data System gravity field products, typically available with a latency of 1-2 months. The QL data are useful to assess gravity changes by earthquakes and examine early seismic models and tsunami models with large uncertainty. For the 2010 Maule earthquake, we used single pass data (L1B) to distinguish between early coseismic slips models but this data was not available until more than a month after the event . The following figure compares the QL data with the final release (V04) data in range-rate (left) and range-acceleration (right) between two satellites and shows the difference of the QL data from the final one is less than the measurement noise (*Han et al.,* 2021).

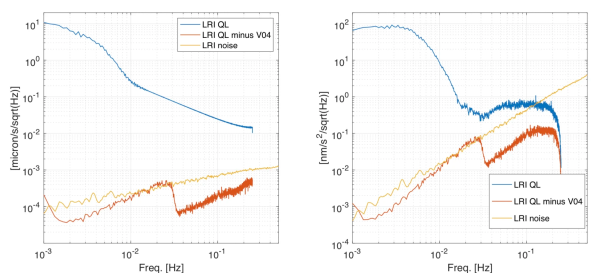

GRACE FOLLOW-ON GRAVITY MEASUREMENTS (CONT'D)

The following figures show the actual gravity change data (LGD time series) along the orbital tracks across the area including the Chignik earthquake rupture. The background map shows the synthetic gravity change computed with the GCMT solution (https://www.globalcmt.org/). Three days of ascending tracks and three days of descending tracks are shown. Blue indicates laser measurements every second and red curve shows the expected GCMT gravity signals along the tracks. The change is the residual from the mean gravity field computed with the data from 1st to 28th of July 2021, just before the earthquake on 29th of July. N.B. these LGD data can be available within a few days of the event.

Ascending track data

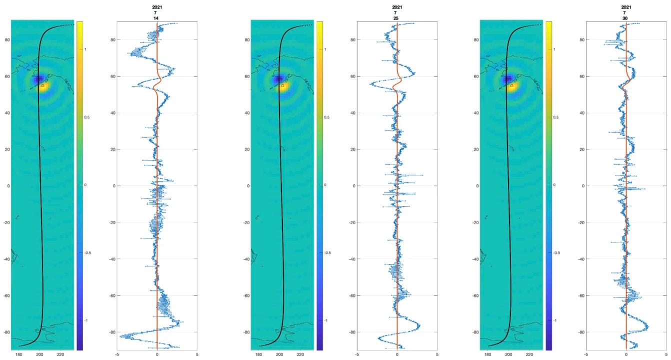

Descending track data

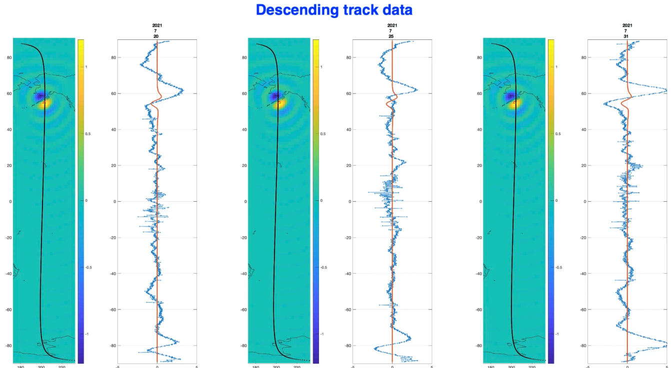

In both cases, the GRACE-FO measurements show largest day-to-day variability (a few nm/s^2) in high latitude regions; specifically, the Ross iceshelf and Alaska. The large ocean tidal mass changes in the Bristol Bay, Alaska (>6 m tidal elevation range near the coast) and beneath the Ross iceshelf and Alaskan glacier mass variability seem dominant in the GRACE-FO measurements. These signals are complicating the interpretation of the gravity observations over the Chignik area. However, the earthquake gravity perturbation (1-2 nm/s^2) is certainly above the general measurement threshold based on earlier experience.

POSTSEISMIC (VISCOELASTIC) GRAVITY CHANGE

The Earth's mantle responds immediately to stress change caused by earthquakes and continues for at least years to decades. The schematic below shows how viscoelastic vertical motions differ by source for full or partial rupture of the lithosphere. Vertical motion is a dominant source of gravity change during the postseismic phase (i.e., volume change is insignificant).

Melosh [1983]

The boundary condition rules!

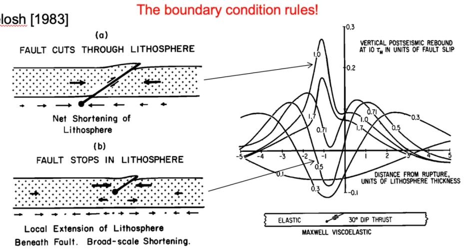

=> Regional uplift (from GRACE) on top of local subsidence (from GPS) is a characteristic feature of the viscoelastic vertical motion with the partially-ruptured elastic lithosphere.

=> A combined analysis of GRACE and GPS constrains the relative thickness of the elastic lithosphere to the rupture depth.

The simulated cumulative gravity changes were evaluated at 10 years after the event for two different cases. With a 40 km thick lithosphere and 10^{18} Pa s asthenosphere viscosity, the postseismic gravity change could be as large as 5-6 microGal. This is due to viscoelastic vertical uplift by several cm over 10 years at 400 km spatial scale.

Postseismic (viscoelastic) gravity change: Modeling

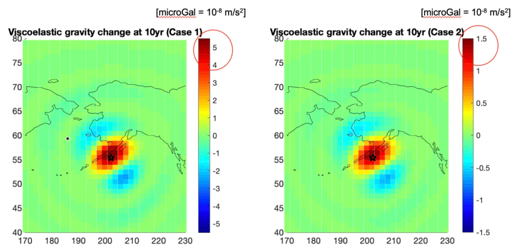

Case 1
Lithosphere thickness = 40 km
Asthenosphere viscosity = 10^{18} Pa s

Case 2
Lithosphere thickness = 80 km
Asthenosphere viscosity = 5×10^{18} Pa s

1 microGal = ~1 cm crustal uplift @ 400 km scale

The postseismic gravity change from a similar magnitude event sequence (M_w8.3, 8.1 2006/7 Kuril Islands doublet, *Han et al.,* 2016.) presented 5 microGal of gravity changes over 14 years measured by GRACE & GRACE-FO. This observation is modeled by viscoelastic relaxation with 40 km thick lithosphere and 10^{18} Pa s viscosity as shown below:

Postseismic (viscoelastic) gravity change:
Examples from 2006/2007 M_w8.3 Kuril earthquake

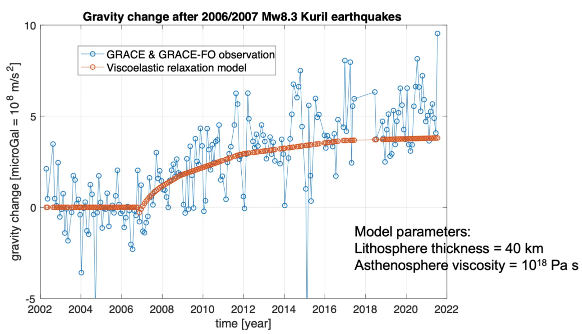

ABSTRACT

This paper presents a new method of analyzing gravity change associated with the solid Earth deformation by earthquakes such as the M 8.2 Chignik event . The vertical deformation and density change after earthquakes result in changes in the Earth's gravity field that are detectible by GRACE and GRACE Follow-On (GRACE-FO) spacecraft. Our approach exploits instantaneous gravity perturbation measured by the intersatellite ranging systems between two GRACE Follow-On satellites for early detection, with 1-3 days of latency after the event. This method can be particularly useful for assessing and distinguishing between early models of earthquake fault slip.

The M_w 8.2 Chignik earthquake is near the coseismic detection threshold estimated during the earlier GRACE (2002-2017) and the current GRACE-FO (2018-present) gravity and mass change satellite missions. The GRACE-FO mass change satellites include the higher-precision Laser Ranging Interferometer (LRI) in addition to the microwave (K-/Ka-band) instrument. However, a particular challenge for the Chignik event is that the Gulf of Alaska is poorly modeled with existing ocean correction models such as Atmosphere and Ocean De-aliasing (AOD) model currently used by the GRACE and GRACE-FO project.

Two other subduction zone sequence of earthquakes of similar magnitude, the 2006-2007 Kuril events (M_w 8.3 & 8.1) and the 2009 Tonga-Samoa (M_w 8.1) complex event, exhibited large, long-wavelength post-seismic mass changes that were detectable by the GRACE and GRACE-FO data. Both cases produced on-going gravity changes that can be accounted for by viscoelastic relaxation. In fact, the cumulative gravity change over several years exceeded the coseismic gravity change. It is, therefore, anticipated that the M_w 8.2 Chignik event will likely yield significant postseismic gravity perturbation as well. In addition to the magnitude and distribution of fault slip, the post-seismic signal depends on the elastic lithosphere thickness and viscosity of the asthenosphere. Post-seismic relaxation following the earlier, nearby 2020 (M 7.8 & 7.6) earthquakes may contribute to the gravimetric signal as well. We will present our early results of the predicted gravity changes after the M_w 8.2 Chignik earthquake. Additionally, we will discuss what can be improved for timely detection of the gravity change signature and how we can use gravimetric data for a unique perspective on the subduction zone process.

REFERENCES

Broerse, T., R. Riva, W. Simons, R. Govers, and B. Vermeersen (2015), Postseismic GRACE and GPS observations indicate a rheology contrast above and below the Sumatra slab, *J. Geophys. Res.* Solid Earth, 120, doi:10.1002/2015JB011951.

Han, S-Ch, J. Sauber, and S. Luthcke, 2010, Regional gravity decrease after the 2010 Maule (Chile) earthquake indicates large-scale mass redistribution,*Geoph. Res. Lett.,* https://doi.org/10.1029/2010GL045449.

Han, S-Ch, J. Sauber, and F. Pollitz, 2016, Postseismic gravity change after the 2006–2007 great earthquake doublet and constraints on the asthenosphere structure in the central Kuril Islands, *Geophs. Res. Lett.,* https://doi.org/10.1002/2016GL068167 (https://doi.org/10.1002/2016GL068167)

Han, S.-C., I.Y. Yeo, M. Khaki, C.M. McCullough, E. Lee, & J. Sauber, 2021. Novel along-track processing of GRACE Follow-On laser ranging measurements found abrupt water storage increase and land subsidenceduring the 2021 March Australian flooding. *Earth and Space Science,* 8, e2021EA001941. https://doi.org/10.1029/2021EA001941

Melosh, H. J., 1983, Vertical movements following a dip-slip earthquake, *Geophys. Res. Lett.,* 337, 10, 47–50, doi:10.1029/GL010i001p00047.

LINK TO A SURVEY

Enter your survey URL here

https://example.com

Submit

Delete